RESEARCH ARTICLE

S. B. Bortolami · S. Rocca · S. Daros
P. DiZio · J. R. Lackner

Mechanisms of human static spatial orientation

Abstract We have developed a tri-axial model of spatial orientation applicable to static 1g and non-1g environments. The model attempts to capture the mechanics of otolith organ transduction of static linear forces and the perceptual computations performed on these sensor signals to yield subjective orientation of the vertical direction relative to the head. Our model differs from other treatments that involve computing the gravitoinertial force (GIF) vector in three independent dimensions. The perceptual component of our model embodies the idea that the central nervous system processes utricular and saccular stimuli as if they were produced by a GIF vector equal to 1g, even when it differs in magnitude, because in the course of evolution living creatures have always experienced gravity as a constant. We determine just two independent angles of head orientation relative to the vertical that are GIF dependent, the third angle being derived from the first two and being GIF independent. Somatosensory stimulation is used to resolve our vestibular model's ambiguity of the up–down directions. Our otolith mechanical model takes into account recently established non-linear behavior of the force–displacement relationship of the otoconia, and possible otoconial deflections that are not co-linear with the direction of the input force (cross-talk). The free parameters of our model relate entirely to the mechanical otolith model. They were determined by fitting the integrated mechanical/perceptual model to subjective indications of the vertical obtained during pitch and roll body tilts in 1g and 2g force backgrounds and during recumbent yaw tilts in 1g. The complete data set was fit with very little residual error. A novel prediction of the model is that background force magnitude either lower or higher than 1g will not affect subjective vertical judgments during recumbent yaw tilt. These predictions have been confirmed in recent parabolic flight experiments.

Keywords Spatial orientation · Otolith organs · Somatosensation · Subjective vertical · Gravity · Orientation model

Introduction

Spatial orientation is typically studied by exposing subjects to body tilt and translation in high and low background acceleration levels and measuring factors such as thresholds for detection of motion, the apparent visual vertical, the self-vertical, auditory and visual target localization, or postural and oculomotor responses. In the 1950s and 1960s, a number of attempts were made to model orientation in terms of underlying vestibular mechanisms. Mayne (1950, 1974) likened the vestibular organs to an inertial guidance mechanism with the semicircular canals serving as tri-axial rate gyros and the otolith organs as linear accelerometers. Young and his colleagues developed a multisensory model of orientation in which vestibular, neck proprioceptive, and visual information were interrelated to generate orientation estimates (Young et al. 1966; Meiry 1966; Meiry and Young 1967). Ormsby (1974) and Ormsby and Young (1976, 1977) extended this approach. The Ormsby and Young model used ratios of the forces detected along the three axes of the otolith organs to determine the orientation of the head with respect to gravity or to gravitoinertial force (GIF). With suitable adjustment of gains and non-linearities among the different axes, the model could reproduce many orientation phenomena, for example, the Aubert

S. B. Bortolami (✉) · S. Rocca · S. Daros · P. DiZio
J. R. Lackner
Ashton Graybiel Spatial Orientation Laboratory MS 033,
Brandeis University, Waltham, MA 02454-9110, USA
E-mail: Simborto@brandeis.edu
Tel.: +1-781-7362033
Fax: +1-781-7362031

P. DiZio · J. R. Lackner
Volen Center for Complex Systems, Brandeis University,
Waltham, MA 02454-9110, USA

(A) and Müller (E) effects[1]. Later models of vestibular dynamics incorporated the concept of an internal model (e.g. Oman 1982) based on extending to human spatial orientation emerging concepts in control theory and optimal estimation (cf. Kalman 1960). Many recent approaches of this kind use "sensory integration" (cf. Merfeld 1995; Merfeld et al. 1999; Zupan et al. 2002; Glassauer and Merfeld 1997; Angelaki et al. 1999; Bos and Bles 2002) to produce an internal estimate of body position and orientation.

Our model does not describe response dynamics but deals with the static orientation of the perceived GIF with respect to the head during steady-state conditions. The approach we present here goes back to ideas that pre-dated tri-axial models which fully reproduce GIF direction and magnitude. Our approach is a natural extension of the pioneering observations of Correia et al. (1968) who showed that the ability to judge the upright is best described as a function of the ratio of shear forces on the utricles and saccules. A key biological perspective of our approach is that humans and other animals evolved under conditions in which the GIF vector departed in magnitude from 1g only transiently, such as during running or jumping. Therefore, *prima facie* orientation mechanisms might have evolved in an economical fashion by taking the magnitude of the background force of gravity as a non-changeable entity.

Taking this as an assumption leads to at least four important implications for the structure of the perceptual component of our mathematical model. The first is that the sensed components of the physical GIF will be interpreted as being the outcome of 1g gravity in all situations, even for example, in modern vehicles where the human body is exposed to GIFs larger or smaller than 1g. The second is that only two components of the gravity vector are sufficient to estimate the direction of the GIF with respect to the head. (We explain later what projections these are.) These implications lead to predictable patterns of orientation errors when the GIF departs from 1g. The third is that identical predictions will be produced by an upward or downward gravity vector; therefore, an independent non-vestibular input is needed to differentiate "up" from "down". The fourth is that somatosensation is used to resolve this ambiguity. Throughout evolution the direction of "down" has been associated with the part of the body surface in contact with the ground resisting the acceleration of gravity.

Recent developments have provided the opportunity for us to incorporate the mechanics of otolith transduction of GIF projections into our model. Grant and Best (1987) and Kondrachuk (2001) have shown that otolith non-linearities and cross-talk might exist. Our model attempts to predict orientation errors in different GIF environments that arise from such otolith transduction errors as well as from our hypothesis, formulated above, that the CNS assumes the GIF is always equal to 1g in magnitude. In summary, the static orientation model to be described includes an otolith mechanosensory component, a vestibular computational component, and a minimal somatosensory component. The free parameters of the model are associated with the mechanosensory model embedded in the computational model.

Static orientation models have been primarily developed to account for orientation in pitch and roll relative to gravity because these axes define upright body posture as well as the desired attitudes of spacecraft and aircraft. In this paper, we will extend predictions of judgments of static body orientation with respect to the gravitational vertical to all three canonical axes: pitch, roll and recumbent yaw. The free parameters of the integrated mechanical/perceptual model were determined by fitting it to a composite data set where the GIF varied on three axes. We measured subjects' ability to indicate the gravitational vertical when tilted in pitch, in roll, and in yaw while recumbent in a normal 1g environment. Details about the experiment and the data are presented in the companion paper (Bortolami et al. 2006). We also made use of literature data on orientation judgments in roll and pitch for GIF levels greater than 1g (Correia et al. 1968; Miller and Graybiel 1964). The fitted model predicts pitch, roll, and recumbent yaw performance in variable GIF environments. One novel prediction of the model is that perceived head orientation in yaw with the body recumbent will not be affected by GIF magnitude whereas it will be for the pitch and roll axes.

Methods

Reference frames and terminology[2]

The otoconia of the otolith organs are acted on by gravity (**g**) and by linear acceleration (**a**) of the body. The gel layers of the otolith organs exert constraint forces that limit the displacements of the otoconia. These forces are collectively equal to $m(\mathbf{g}-\mathbf{a})$, where m is the total mass of the otoconia. The exact value of the mass, m is generally not known, but is not strictly needed since we can use the quantity:

$$\mathbf{f} = \mathbf{g} - \mathbf{a} \tag{1}$$

known as the "specific force" (cf. Savage 2000); **f** has properties akin to force (GIF), but is dimensionally an

---

[1]The Aubert effect represents an underestimation of body tilt in judging the visual vertical; the Müller effect is the overestimation of body tilt in judging the visual vertical (cf. Schöne 1964; and Howard and Templeton 1966).

[2]We indicate a vector with a boldface character like **p** ($\mathbf{p} \in \Re^3$), its components with p_i, ($p_i \in \Re$), and a scalar with p ($p \in \Re$). Capital boldface characters indicate matrices, e.g., **A** ($\mathbf{A} \in \Re^{l \times q}$).

acceleration. The specific force **f** can be seen as the force acting upon a unitary "parcel" of otoconia. In the present work, **f** also represents the plumb-bob vertical[3], e.g., the combination of gravity and centrifugal force.

The input to our mathematical model is "body orientation" relative to vector **f**, and the output is the "perceived direction" of the internal estimate of **g** relative to the body. The orientation of the head with respect to the GIF produces force components along the cardinal axes of the head. These components are then entered in the model to produce the "perceived orientation", see Appendix for details. These quantities are defined in the head frame of reference (occipito-nasal, i_1; right-left, i_2; and base-vertex, i_3) as illustrated in Fig. 1a. They are sensed, however, by the otoliths along the specific "planes" of the utricles and saccules. We adopt a simplified geometry of the layout of these organs with respect to the head, namely, that the saccular and utricular planes intersect orthogonally at the i_2 (right-left) axis and are both tilted 30° back with respect to the head horizontal orientation as illustrated in Fig. 1a (cf. Wilson and Melvill Jones 1979). The otolith frame of reference is denoted i'_1, i'_2 and i'_3 ($i'_2 \equiv i_2$).

Estimation of head roll and pitch

A classic idea first explored by Schöne (1964) was that head orientation with respect to gravity could be inferred from the shear force u produced by gravity onto the utricles (see Fig. 2), which is a sine function of the orientation angle φ_R. However, Correia et al. (1964) obtained data on roll and pitch orientation in 1 and 2g environments that did not support an orientation scheme based on $\sin^{-1}(u)$. Correia et al. suggested a scheme based on a transformation associated with the tangent of the angle, and they proposed that this quantity represents the projection of the GIF vector onto a spatially horizontal plane. The first postulate of our model is that the CNS processes otolith signals related to this quantity, p_R where:

$$p_R = f \cdot \tan(\varphi_R) \tag{2}$$

The quantity p_R, which is illustrated in Fig. 2 is central to our model. The projection p_R, is the result of the decomposition of the vector **f** along the i'_3 axis and the plane orthogonal to **f**.

The second postulate of our model is that p_R is interpreted by the CNS as being produced by 1g gravity. Another way of expressing this is to say that the

magnitude of the gravity vector is not computed and that any GIF is treated as if $f \equiv g$. Consequently, we may write the non-linear transformation that produces the physiological estimate of head roll $\hat{\varphi}_R$ from p_R as follows (the symbol "^" indicates "estimate"):

$$\hat{\varphi}_R \triangleq \tan^{-1}\left(\frac{p_R}{g}\right). \tag{3}$$

The force p_R can be estimated from quantities sensed by the otolith organs. For roll tilts, p_R has components in the i'_2 and i'_3 axes of the simplified otolith organs (see Fig. 1). Within the reference frame of the otolith organs (i'_1, i'_2, i'_3), the mechanical stimulus[4] $f' = (f'_1, f'_2, f'_3)$ produces displacements of the otoconia x'. These displacements lead to proportional neuronal discharges and internal representations $\tilde{x}' = (\tilde{x}'_1, \tilde{x}'_2, \tilde{x}'_3)$, which are indicated with the "~". We assume that these quantities encoding otoconial displacements are mapped to the head reference frame before entering further stages of computation. Figures 2 and 3 omit this remapping, for the sake of visual clarity, but it is discussed later on where it is implemented in our working model (see Eq. 13). We formalize these assumptions with the following relationships:

$$f \cdot \sin\varphi_R \propto \tilde{x}_2, \quad f \cdot \cos\varphi_R \propto \tilde{x}_3, \tag{4}$$

where $\tilde{x}_2$ and $\tilde{x}_3$ are the encoded otoconial displacements transformed into the head frame (cf. Fig. 2). Inserting Eq. 4 in Eq. 2 and in turn into Eq. 3 we obtain the following expression for estimating the roll angle of the head.

$$\hat{\varphi}_R = \tan^{-1}\left(\frac{f}{g} \cdot \frac{\tilde{x}_2}{\tilde{x}_3}\right). \tag{5}$$

Equation 5 involves f/g, the ratio between the specific force of the stimulus and the gravitational force. In higher or lower than 1g environments f will be different from 1g. This is the main algorithmic consequence of postulating that projections of the GIF vector are interpreted as if they were produced by 1g acceleration, see the Appendix for additional details.

The same considerations underlying the estimation of roll can be made for determining orientation in pitch ($p_P = -f \cdot \tan(\varphi_P)$). For pitch, we obtain the following relationship:

$$\hat{\varphi}_P \triangleq \tan^{-1}\left(\frac{f}{g} \cdot \frac{-\tilde{x}_1}{\tilde{x}_3}\right). \tag{6}$$

Estimation of recumbent yaw tilt of the head

Our model mathematically constructs a representation of the gravity vector with respect to the head. As a result

---

[3] The human otolith organ has an estimated static resolution of about 0.25 m s^{-2} (Graybiel and Patterson 1955). Newton in 1686 showed within 1 part per thousand that gravitational mass and inertial mass are equivalent. In 1972, Barginsky and Panov showed that these two masses are equivalent within 1 part per trillion (cf. Will 1981). This experimental evidence was later embraced by Einstein as a principle (not a law) in his theories. Consequently, the human otolith organ, which operates on displacements of the otoconia *cannot* differentiate between gravity and inertial forces.

[4] $(f'_1, f'_2, f'_3) = R_y(-30)^T \cdot f$; $R_y(\pm 30) \in SO(3)$ is the transformation matrix between the head and otolith reference frames; see Murray et al. (1994); $R_y^{-1} = R_y^T$; see Appendix.

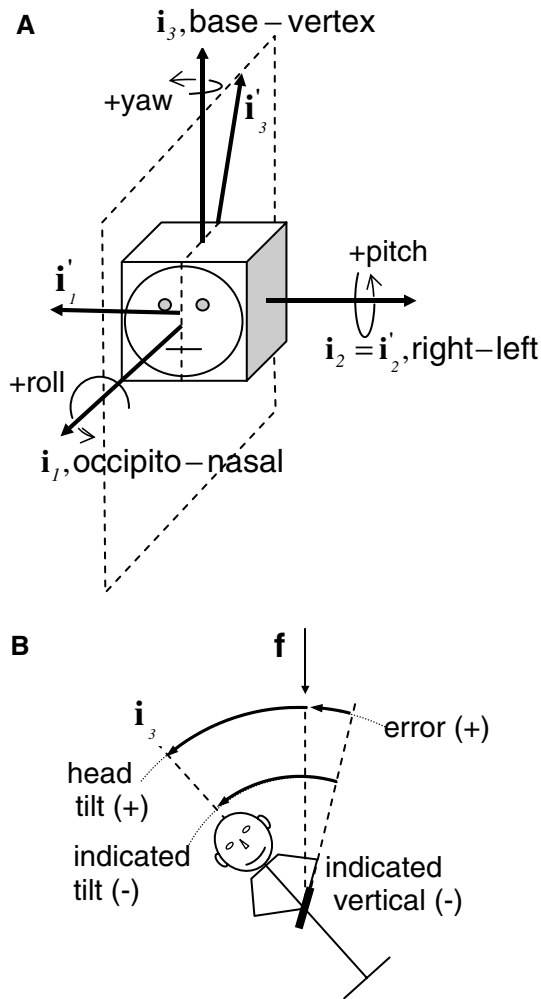**Fig. 1 a** Definition of the head coordinate frame (occipito-nasal axis, $\mathbf{i}_1$, right–left axis, $\mathbf{i}_2$, and base–vertex, $\mathbf{i}_3$). The $\mathbf{i}_1$–$\mathbf{i}_2$ plane will be referred to as the transverse plane. Otolith coordinate frame ($\mathbf{i}'_1$, $\mathbf{i}'_2$, $\mathbf{i}'_3$); head and otolith frames share the axis $\mathbf{i}_2 \equiv \mathbf{i}'_2$ (right–left). **b** Diagram, for the case of roll tilt, of the calculation of haptically indicated vertical and of errors in haptically indicated vertical

of our postulate that the CNS assumes **g** to be constant in magnitude, two angles suffice for determining the **g** direction. The first angle, the elevation of the gravity vector with respect to the head's transverse ($\mathbf{i}_1$–$\mathbf{i}_2$) plane, has been dealt with above for the cases of pure roll and pitch tilts. The other angle needed is the azimuth angle of the GIF projection onto the transverse plane with respect to the $\mathbf{i}_1$ and $\mathbf{i}_2$ axes. In our model, azimuth is calculated as the ratio of the two quantities p_P and p_R already used for the roll and pitch cases, as follows:

$$\hat{\varphi}_Y \triangleq \tan^{-1}\left(\frac{p_R}{p_P}\right) = \tan^{-1}\left(\frac{\tilde{x}_2}{\tilde{x}_1}\right). \tag{7}$$

In the particular case of pure recumbent yaw orientation, which we have experimentally tested, the GIF acts in the head's transverse plane and $\hat{\varphi}_Y$ is the main angle determining the orientation of the GIF. An important
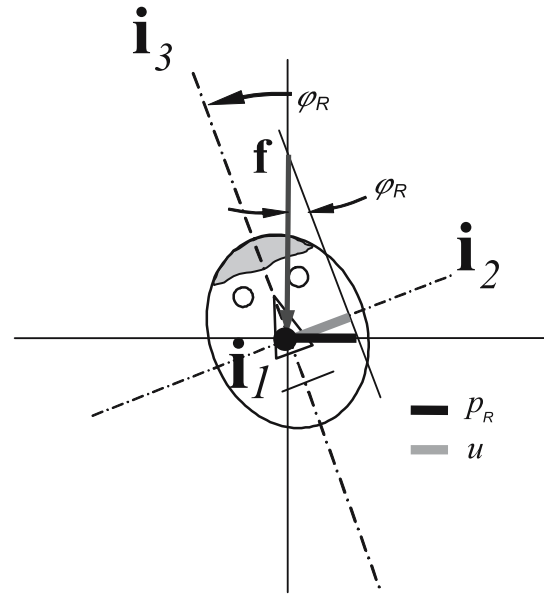

Fig. 2 The variables involved in the perception of tilt in roll. ϕ_R represents the actual body roll angle relative to the gravitoinertial resultant vector, **f**. u is the projection of f onto the right-left ($\mathbf{i}_2$) axis; p_R is the projection of $\mathbf{f}$ along the $\mathbf{i}'_3$ axis onto a plane orthogonal to **f**. The model postulates that p_R rather than u is processed as if it were generated by $\mathbf{f} \equiv \mathbf{g}$, where **g** is the acceleration of gravity

consequence of Eq. 7 is the prediction that perception of head orientation during pure recumbent yaw tilts is independent of the stimulus level f/g.

General case of estimation of head orientation with respect to gravity

In the preceding sections, we introduced the rationale for our model using cases involving pure rotations about the three canonical axes. Here, we extend the algorithm, the perception model, to the general case of a tri-dimensional tilt of the head with respect to the GIF (**f**), which we have implemented numerically, see Fig. 3. The variables are here redefined as follows for convenience of numerical implementation.

$$\hat{\varphi}_{RP} \triangleq \tan^{-1}\left(\frac{f}{g} \cdot \frac{\sqrt{\tilde{x}_1^2 + \tilde{x}_2^2}}{-\tilde{x}_3}\right). \tag{8}$$

$$\hat{\varphi}_Y \triangleq \tan^{-1}\left(\frac{\tilde{x}_2}{\tilde{x}_1}\right) \tag{9}$$

where $\hat{\varphi}_{RP}$ represents the complement to the gravity elevation angle, which for pure roll or pitch tilts becomes $\hat{\varphi}_R$ or $\hat{\varphi}_P$. $\hat{\varphi}_Y$ represents the azimuth of the gravity vector.[5] The perception model's output is the internal

---

[5] The round hat indicates an estimate like the triangular hat. A different symbol was needed to differentiate the two formalisms for the estimation of φ_Y. Details are presented in the Appendix.
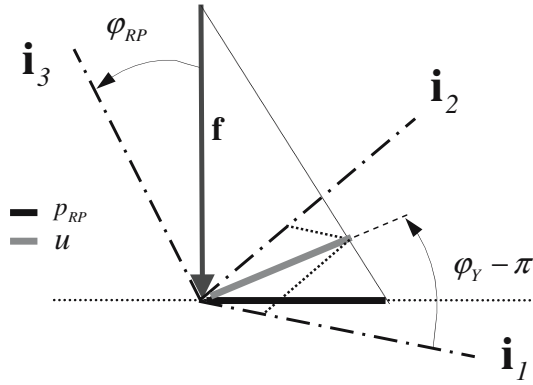
Fig. 3 Variables involved in the perception of tilt in roll, pitch, and recumbent yaw: φ_{RP} represents the actual body roll/pitch angle or elevation angle; p_{RP} represents the tangent to the angle φ_{RP}; φ_Y is the azimuth angle or recumbent yaw tilt; u is the projection of the GIF onto the transverse ($\mathbf{i}_1$–$\mathbf{i}_2$) plane of the head; see text for further detail. The figure extends to three dimensions the variables introduced by Fig. 2

representation of the perceived gravity vector with respect to the head reference frame. The estimate of $\mathbf{g}$ is represented as follows: $\hat{\mathbf{g}} \triangleq \{\sin(\widehat{\varphi}_{RP})\cos(\widehat{\varphi}_Y),$ $\sin(\widehat{\varphi}_{RP})\sin(\widehat{\varphi}_Y), -\cos(\widehat{\varphi}_{RP})\}$. For numerical purposes in order to compare the model's output of perceived orientation with experimental data on perceived orientation, we used the projection angles of $\hat{\mathbf{g}}$ onto the head axes; see Appendix for details and numerical implementation of the model.

Haptic contribution to orientation

The central hypothesis of our vestibular perception model is that only two projections of the gravity vector with respect to the head are used to estimate the direction of the gravity vector. Because such an estimate cannot distinguish upright orientations from inverted orientations an additional source of information is necessary. Our third postulate is that spatial mechanisms distinguish the true orientation of the gravity vector by means of "seat of the pants" or equivalent haptic information. We address this issue further in the Discussion section. We have incorporated this role of somatosensation by extending Eqs. 8 and 9 to four quadrants, as explained in the Appendix, by using four quadrant arctangent functions (MATLAB atan2 function).

However, because of the work of Graybiel and Patterson (1955), Brown (1961), and Kaptein and Van Gisbergen (2004), we recognize that spatial orientation may be less precisely specified when the body is inverted. We have limited the present study to non-inverted orientations and have postulated that vestibular and somatosensation signals jointly participate in the estimation of the gravity vector, with the primary role of the vestibular system in determining body angle in relation to gravity and the primary role of somatosensation in determining the direction of up and of down.

Mechanics of the otolith organs

The utricle and saccule have gel layers in which the otoconia are embedded. The cilia of the receptor neurons are also embedded in the lower third of the gel layers. Under the action of gravity and inertial forces, the otoconia and gel are displaced laterally deflecting the cilia trapped within the gel. The deflections of the cilia affect the generator potentials of their parent neurons and determine their discharge rates (Fernandez et al. 1972; Wilson and Melvill Jones 1979). Grant et al. (1987, 1994) have hypothesized that as displacement magnitude increases the gel layers become more rigid and as a consequence the resulting neural response is not linearly related to shear force magnitude. The otoliths also are not flat membranes but have a three dimensional organization (cf. Spoendlin 1965; Wilson and Melvill Jones 1979). Consequently, when otoconia are deflected in one direction by gravitational or inertial forces they may also shift in another direction. Kondrachuk (2001) showed a similar effect solely due to action of the gel layer (reaction of the stretched substrate) on the guinea pig utricle. It is necessary to take into account such inherent aspects of otolith mechanics in modeling experimental data. Details are presented in the Appendix and the Discussion section.

We modeled the otolith sensors as follows:

$$\tilde{\mathbf{x}}' = \mathbf{A}\mathbf{f}' + \mathbf{B}(\mathbf{f}')^n, \tag{10}$$

where the matrices $\mathbf{A}$ and $\mathbf{B}$ are composed of compliance terms. In particular, $\mathbf{A}$ and $\mathbf{B}$ have the following form:

$$A = \begin{bmatrix} a_{11} & 0 & a_{13} \\ 0 & a_{22} & 0 \\ a_{31} & 0 & a_{33} \end{bmatrix} \quad B = \begin{bmatrix} b_{11} & 0 & b_{13} \\ 0 & b_{22} & 0 \\ b_{31} & 0 & b_{33} \end{bmatrix},$$

with $a_{13} = a_{31}$ and $b_{13} = b_{31}$ (nine free model parameters). The stimulus $\mathbf{f}' = (f'_1, f'_2, f'_3)$ is in otolith coordinates. The output $\tilde{\mathbf{x}}'$, also in otolith coordinates, represents the combined displacement of the otolithic maculae along the three cardinal axes (the left and right otolithic maculae are combined with equal weights). The output $\tilde{\mathbf{x}}'$ is transformed into head coordinates by means of $\tilde{\mathbf{x}} = \mathbf{R}_y(-30) \cdot \tilde{\mathbf{x}}'$, where $\mathbf{R}_y$ (± 30) $\in$ ESO(3). Entering the quantities $\tilde{\mathbf{x}}$ into the "perception model", Eqs. 8 and 9, we obtain the full orientation model. See Appendix for further details.

Data platform and fitting of model parameters

In the preceding companion paper, we collected orientation data with respect to gravity for all three axes, roll, pitch, and recumbent yaw (Bortolami et al. 2006). Subjects aligned a pointer with the perceived vertical, as illustrated in Fig. 1b. The haptically indicated tilt data are shown in Fig. 4. Other investigators had collected data on the pitch and roll axes, and our haptic

measurements were compatible for comparable test conditions with theirs obtained with visual and haptic indicators. For model fitting, we used our comprehensive 1g data set and augmented it with the 2g data sets available for pitch (Correia et al. 1968) and roll (Miller and Graybiel 1964).

Our model and many other models in the literature as well as anatomical studies assume the vestibular organs are symmetrical, on average across subjects, with respect to the sagittal plane. Therefore, roll and recumbent yaw data are expected to be symmetric with zero bias, except of course in cases of pathology. Our raw data contained only minor asymmetries and zero biases. Before the fitting procedure, the roll data (1g and 2g) and recumbent yaw data (1g) were symmetrized by averaging the measurement points on the two opposite quadrants of graphs and zero biases were removed, for each subject individually (cf. the companion paper, Bortolami et al. 2006, for further details on symmetrization). Pitch data are not expected to be symmetric nor to have zero bias. The saccular and utricular planes have no structural symmetry about the head's inter-aural axis and are pitched back approximately 30° relative to the head. Therefore, we did not symmetrize the pitch data nor remove zero biases. The medians and interquartile ranges, across subjects, of the raw pitch data and of the symmetrized, unbiased roll and yaw data are graphed in Fig. 4.

The data for all three axes and both GIF levels were used to identify coefficients of our model, the matrices **A** and **B** and the exponent n in Eq. 10, which generated the closest fit to the data. The model fitting was accomplished using least squares minimization of predicted values of perceived orientation in comparison to the subjects' indications. Predicted values were computed using Eq. 10 and then integrated into the perception model of Eqs. 8 and 9. All data sets, treated as described above, and predictions were expressed as perceived tilt at each body tilt relative to the vertical (**f**), see Fig. 4. The Appendix describes in more detail the rationale and methods for the fitting procedure.

In this article, as is typical in the literature (e.g. Correia et al. 1968; Van Beuzekom and Van Gisbergen 2000), we focus on error patterns between perceived and predicted tilt as a function of actual tilt angles, even though the model output is orientation of the head. This approach allows us to discuss and analyze results in terms of underestimation/overestimation of the perceived body orientation angle with respect to the actual angle relative to the gravitational vertical. If a subject indicated the perceived vertical in a location to the other side of the true vertical (**f**) as his or her body (see Fig. 1b), we assumed that he/she felt more tilted than actually was the case (cf. also Howard and Templeton 1966). If a subject indicated the vertical on the same side as his/her body tilt with respect to gravity, we assume that he/she felt less tilted than was the case. In our nomenclature, overestimation of tilt is signified by positive errors for positive tilts and negative errors for negative tilts and vice versa for underestimation. Figure 5 shows the median error patterns for the empirical data and the model errors which were generated by subtracting predicted from actual orientations. To facilitate the interpretation of Fig. 5, we have shaded the underestimation of quadrants to show when subjects feel more tilted than actually is the case.
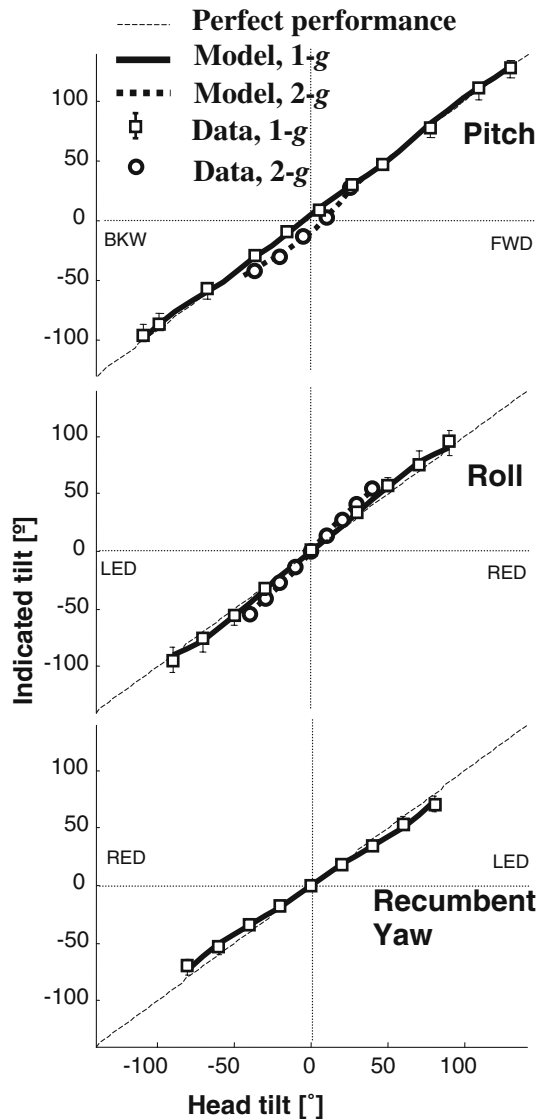

Fig. 4 Static spatial orientation data and model fit: 1g data are from the companion paper Bortolami et al. (2006); the 2g data for roll and pitch performance are re-plotted from Correia et al. (1968) and Miller and Graybiel (1964). Medians and inter-quartile ranges are presented. The acronyms are as follows: left ear down (LED); right ear down (RED); backward (BKW); and forward (FWD)

Results

We identified the coefficients of the matrices **A** and **B** and the exponent n (nine free parameters) that best fit all the spatial orientation data (perceived tilt, not errors)

addressed in the previous section for 1g and 2g on all axes. We report the fitted values of matrices **A** and **B** and of the exponent n in the Appendix

Correlations of perceived and predicted tilt as shown in Fig. 4 yielded r^2 values of approximately one. Figure 5 shows that the model fit of the error data is good for all axes. To quantify the overall model fit to the experimental data, we correlated the actual orientation errors and the model predictions of orientation errors and computed ANOVAs to assess whether significant variance was accounted for by axis and GIF level. The results are: for roll, $r^2 = 0.73$ at 1g ($F = 18.9$) and $r^2 = 0.96$ at 2g ($F = 152.2$); for recumbent yaw, $r^2 = 0.83$ at 1g ($F = 33.6$); and for pitch, $r^2 = 0.53$ for 1g ($F = 10$) and

$r^2 = 0.87$ for 2g ($F = 19.9$). Pitch correlation values of 1g data are low because the error values are very small ($2°$ RMS). However, all correlations and ANOVAs are significant ($P < 0.05$, at least) indicating the model accurately captures the patterns of the experimental errors.

Predictions in pitch follow the 1g data very well over a wide range ($-100°$, $+130°$) as well as 2g data. In addition, the model fit is consistent with the experimental evidence of GIF-independent errors in perceived orientation during 30° pitch forward tilt. In the top panel of Fig. 5, the 1g and 2g model predictions intersect at approximately 30° of forward pitch. This agrees perfectly with the experimental findings of Schöne (1964) and Correia et al. (1968). Roll predictions are also generally in good agreement with the experimental data for both 1g and 2g gravity levels. However, Fig. 5 shows a slight disparity between the model predictions and the 1g data for the extreme roll head tilts. The model predicts a perception error close to zero at 90° of head/body roll while the actual median values are different from zero. A very important result, shown in Figs. 4 and 5, relates to recumbent yaw reorientation. The predicted and perceived yaw orientations match closely over the entire range of body orientations, and more importantly, perception errors for recumbent yaw tilts are predicted to be minimally affected by the level of gravity of the environment. This was anticipated by the formal treatment of the model, and the numerical fit confirmed it. In Figs. 4 and 5 the recumbent yaw predictions of 1g and 2g are practically overlapping. The 2g recumbent yaw traces are predictions of the model, and data from parabolic flight experiments and ground-based centrifugation have confirmed these important predictions (Bryan et al. 2004).

As indicated above, the identification of the model parameters consisted of calculating the matrices **A** and **B** and the exponent n conforming to the experimental data. Identifying these matrices allowed us to probe how the predictions of Grant and Best (1987) would compare with our findings. Grant and Best (1987) theorized that with high shear forces the otolithic response should stiffen (be less compliant). The diagonal terms of matrices **A** and **B** of Eq. 10 predict how a force along each cardinal axis will displace the otoconial mass along that axis. In the case of perfectly linear behavior, the compliance of the mechanical sensor model would be independent of applied force and force vs. displacement would be a straight line. However, because of the nonlinear behavior the input/output compliance of our model varies with the applied force and the force versus displacement departs from a straight line, even though the coefficients of the matrices **A** and **B** are constant. Figure 6 shows the simulated shapes and ranges of otoconia displacements along the three cardinal axes of the otoliths within a range of stimulation of $\pm 3g$. Even though we notice a stiffening (reduced compliance) of the response along the right-left axis, there is a clear prediction of softening (increased compliance) along the
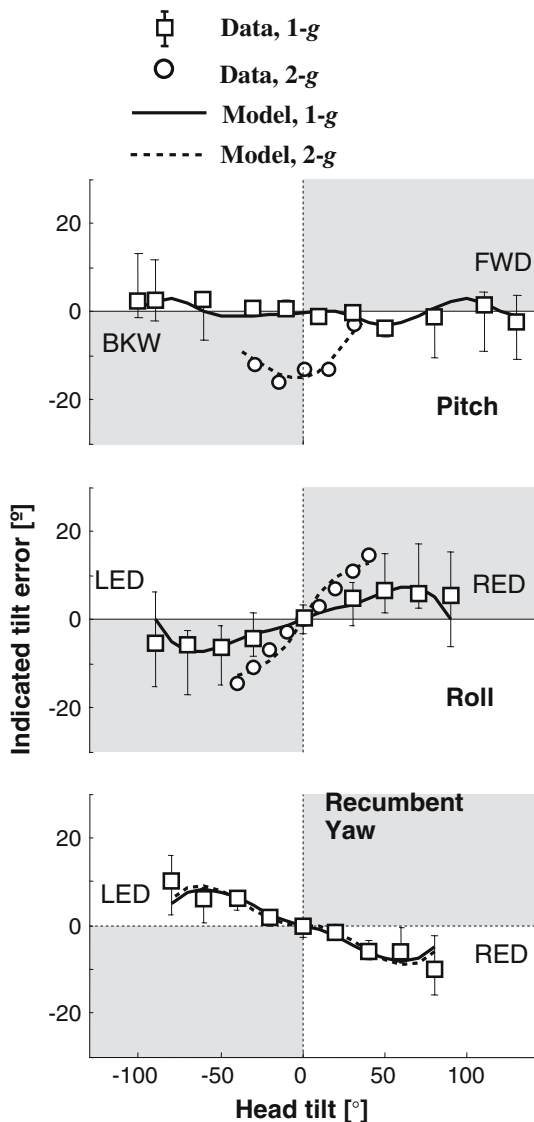

Fig. 5 Medians and inter-quartile ranges of errors in indicated tilt for different body tilt angles relative to gravity in pitch, roll, and recumbent yaw under 1g and 2g conditions. The 2g data for pitch are from Correia et al. 1968, the 2g roll data are from Miller and Graybiel 1964. For acronyms see Fig. 4. The shaded quadrants are where indicated tilts overestimate actual tilt
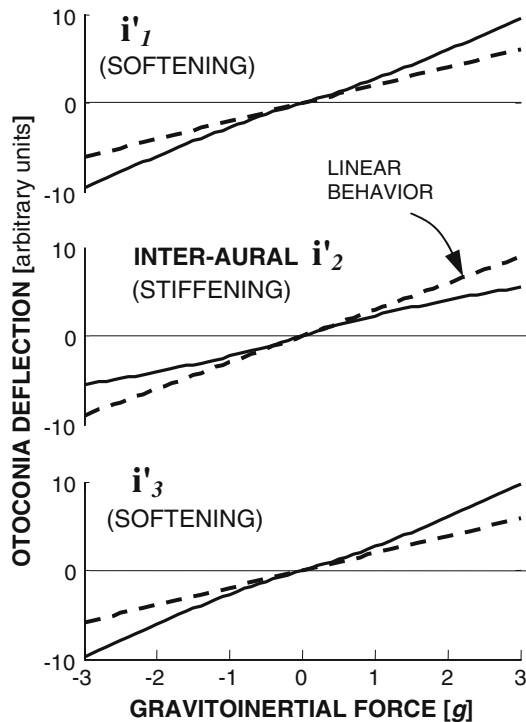
Fig. 6 Softening (increased compliance) and stiffening (reduced compliance) predictions of the model for the sensing characteristics of the otolith organs (*solid lines*). *Dashed lines* indicate the proportional or linear behavior. A *slope higher than that of the dashed line* indicates softening or increased compliance, a *lower slope* indicates stiffening or reduced compliance

base-vertex and occipito-nasal axes, which is in contrast with the Grant and Best (1987) predictions. Finally, because of the tensorial structure of the model, which accounts for cross-talk among axes, the error affecting the estimation $\hat{g}$ has a main component in the plane of head/body tilt as well as a smaller component off the plane of tilt. No study has yet looked for possible off-axis effects but we will do so in future experiments.

Discussion

Several investigators have developed models of static orientation. Correia et al. (1968) derived equations for the roll and pitch axes separately that are very similar to ours using a data fitting approach. No work prior to ours has addressed recumbent yaw orientation. We wanted to formulate a tri-dimensional model of static human spatial orientation as had been the practice for studies of dynamic orientation (Merfeld and Zupan 2002; Haslwanter et al. 2000). We also wanted to ad-dress the issue of cross-talk. The latest dynamic models (e.g. Merfeld et al. 2001; Zupan et al. 2002) assume the otolith matrix to be diagonal, i.e. without cross-talk. Mittlestaedt (1983) developed a model of static orien-tation (the M-model) that employs the concept of an "idiotropic vector". This vector is postulated to be

parallel to the body z-axis and different in magnitude for each subject. Recently Zupan et al. (2002) have incorporated this concept into their dynamic model. The M-model involves the computation of the magni-tude of the GIF stimulus and uses a vector of conve-nient size (a portion of the idiotropic vector), computed from case to case to best fit the data. The idiotropic vector combined with the vestibular estimate of the GIF, can yield A and E error patterns. We, by con-trast, postulate that the CNS assumes gravity cannot change in magnitude and our model uses planar pro-jections of **g** on a spatially horizontal plane to judge relative orientation. This part of our algorithm is responsible for the A and E effects on the different axes in the presence of forces higher or lower than 1g, without the use of other auxiliary vectors.

Subjects with bilateral labyrinthine defects (LD) from injury or disease are of special significance for understanding orientation. LD subjects when blind-folded considerably underestimate their body tilt (Graybiel and Clark 1965). If the estimation of the gravitoinertial vertical with respect to the head relies on a three-dimensional reconstruction of the GIF vector on the basis of a tri-axial measurement by the otolith organs, like in Ormsby and Young (1976, 1977), then LD subjects with some residual function should per-form on average like control subjects, but with higher variability. To understand why this should be the case, consider the examples of a normal and a LD subject each exposed on a centrifuge to a GIF rotated 30° in roll, see Fig. 7. The components of the stimulus for each subject are $\sqrt{3/2}g$ along the z-axis and 1/2g along the y-axis. Assume that the LD subject has a gain of only 20–30% that of the normal subject, a reasonable assumption because ocular counter-rolling, which is dependent on otolith function, was reduced by about 70–80% in the LD subjects tested by Graybiel and Clark (1965) and by Miller et al. (1968). Therefore, for the LD subject, the registered otolith stimulation would be approximately one-third of $\sqrt{3/2}g$ along z and approximately 1/3 of 1/2 g along y. Hence, for the normal and the LD subject the perceived orientation with respect to the GIF derived from these vectors should be equally 30°. One, thus, would expect the performance of the normal and the LD subjects to be similar, but the latter might be noisier.

The set of observations shown in Fig. 8, however, shows major departures in the performance of LD and normal subjects when visual orientation judgments are made during centrifugal rotation (Graybiel and Clark 1965; also Clark and Graybiel 1966). The magnitude of the change in visual horizontal for the LD subjects is only about 30–40% of that of the normal subjects (cf. Fig. 7). These findings are important because they are inconsistent with a head orientation estimation based on assessing the gravity vector in three dimensions, unless utricular and sacular functions degrade differentially in precisely the same manner across LD subjects, but there is no independent evidence of this.
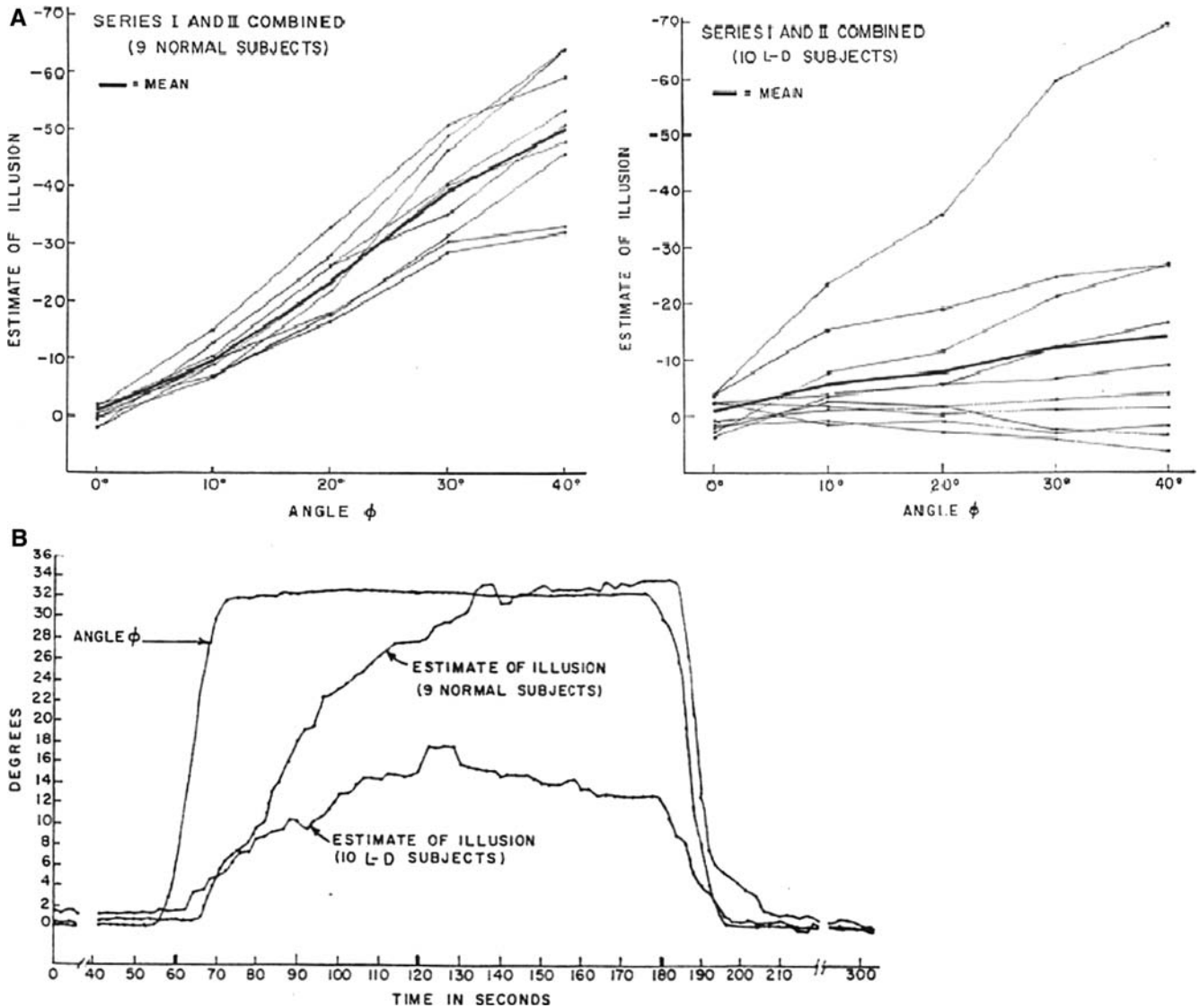
Fig. 7 Magnitude of oculogravic illusion (error in setting a line of light to the apparent horizontal) during exposure to a change in magnitude and direction (angle ϕ) of the gravitoinertial resultant force. **a** The *left graph* shows the performance of nine control subjects; and the *right graph* shows the behavior of ten labyrinthine-defective (*LD*) subjects. **b** *Graphs* show the time course of the illusion in normal and LD subjects. Data are from Graybiel and Clark (1965)

Our model, however, predicts the findings of Graybiel and Clark (1965). We can see from Eq. 3 that if the vestibular system has an output (bilaterally) reduced in gain, p_R would be sensed as smaller in magnitude than it actually is. This is equivalent to having a smaller f/g ratio in Eq. 5. Assuming a value for this ratio of 0.3, we plotted the model's prediction versus the actual Graybiel and Clark (1965) LD data. Figure 9 shows the compatibility of our model predictions and the data for the average LD subject.

Our model relies on horizontal projections of the GIF and the same planar projections are produced either by $+\mathbf{g}$ or $-\mathbf{g}$. We postulate that the CNS uses "seat-of-the-pants" cues to resolve up from down. There is ample support for this postulate. Clark and Graybiel (1968) showed the importance to orientation of mechanical contact cues and active self-support. Lackner and Graybiel (1978a, b, 1979) showed critical influences of somatosensory cues on orientation in weightless as well as 1g environments. Mittelstaedt and Fricke (1988) have evidence that the kidneys may serve as truncal gravitoceptors. This latter finding complements Magnus's classical observations on righting reflexes in blindfolded, labyrinthectomized animals elicited by asymmetric stimulation of the abdomen (Magnus 1924). In our theoretical framework, we assume that the region of body in contact with the ground can specify the direction of "down", but trunk receptors could participate as well. Individuals who are free floating without visual cues often experience an absence of a sense of orientation to their environment. They are cognitively aware of their actual orientation in relation to the vehicle in which
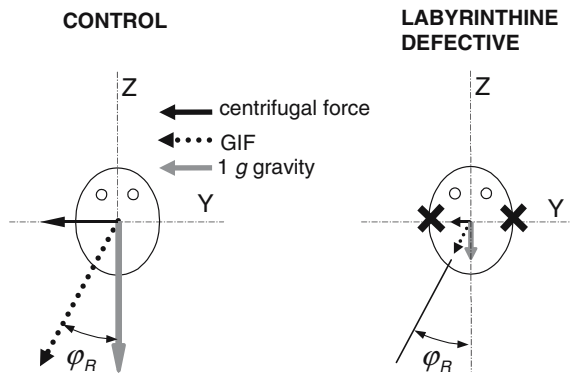
Fig. 8 Most theories of spatial orientation postulate that perception of roll body orientation is determined by the ratio of the magnitudes of the interaural and spinal projections of the gravitoinertial force (*GIF*) on the otolith organs. If this were the case, normal subjects (*left illustration*) and labyrinthine defective subjects with reduced but not absent vestibular function, gain 30% of normal, gain (*right illustration*) should perceive comparable body tilts for a given roll stimulus because the projection ratios would be the same

they are floating, but only experience or sense their relative body configuration (Lackner 1992; Lackner and Graybiel 1979). When tactile cues are applied to the body, these individuals may again experience a sense of "up" and "down", with "down" corresponding to the site of most contact pressure. Similarly, Maxwell (1923) found that blindfolded, labyrinthectomized dogfish swimming upright in an aquarium would on bumping into one of its walls then swim horizontally, taking the contact as indicating the direction of down.

Underwater divers make errors as large as 180° in indicating the vertical when denied visual cues (Brown 1961). Jarchow and Mast (1999) have found that self alignment with the horizontal underwater is also subject to larger errors than on land. Recently, Kaptein and Van Gisbergen (2004) compared 360°-roll-tilt orientation performance against predictions generated using the model developed by Mittlestaedt (1983) and found structural discrepancies between model predictions and performance. This is not surprising because Graybiel and Patterson (1955) demonstrated that subjects when inverted make huge errors in indicating the vertical. In a key experiment, Graybiel et al. (1968) had control subjects and LD subjects indicate the apparent visual horizontal while rotated on a centrifuge under dry conditions and while immersed in water to minimize somatosensory cues. Their findings indicate that perception of the horizontal deteriorates in normal subjects when somatosensory cues are eliminated. Exclusion of somatosensory cues caused an even greater disruption in their LD subjects. An important feature of our model is the prediction that increases in GIF should not affect the perception of the apparent vertical for body tilts in recumbent yaw. This prediction has been fully confirmed in recent parabolic flight experiments (Bryan et al. 2004). This result is incompatible with models that involve tri-axial reconstruction of the GIF direction and magnitude.

Cross-talk and model parameters

Our model accounts for the non-linearity of the otolith organs and their axial cross-talk. The exact origin of the non-linearity and cross-talk is unclear. For example, Grant and Best (1987) posited that the resistance of the gel layer to displacement increases as shear forces increase. Fernandez et al. (1972), recording from otolith afferent units, found that some hair cells respond linearly and others quadratically to increasing deflection. Either one or both of these factors may account for the non-linear behavior of the otolith responses. Similarly, cross-talk could also result from off-axis movement of the otoconia in relation to cell polarization.

Our overall model is non-linear; therefore, model order and parametric sensitivity analyses, which are common practice in linear system identification, are not immediately applicable. The model is composed of a "perception model", Eqs. 8 and 9, and an input–output characterization of the physiological–mechanical properties of the otolith sensors, Eq. 10. The perception model predicts orientation as a function of GIF magnitude. This includes the predictions of a head/body pitch angle at which perception is insensitive to GIF magnitude (see Fig. 5, pitch panels) and the recumbent yaw invariance to the GIF (see Fig. 5, yaw panels). The perception model also predicts the "wavy" nature of the error patterns (e.g., Fig. 5, pitch and roll panels) seen in the experimental data, and the zero-crossing of the roll error pattern at ±90° of roll (cf. Fig. 5, roll panel). Simpler linear models may be adequate for describing one axis at a time, but could not handle the entire three-dimensional, multi-GIF data set.
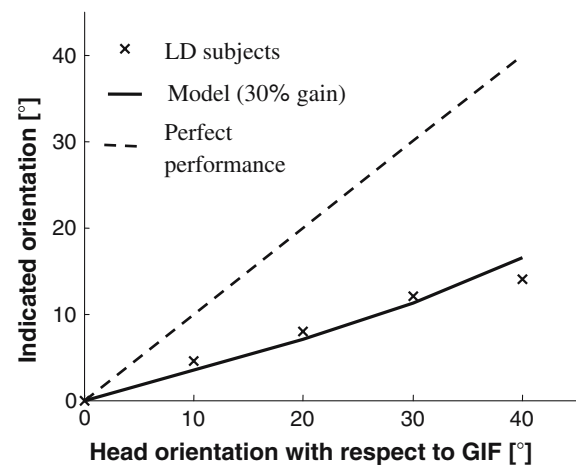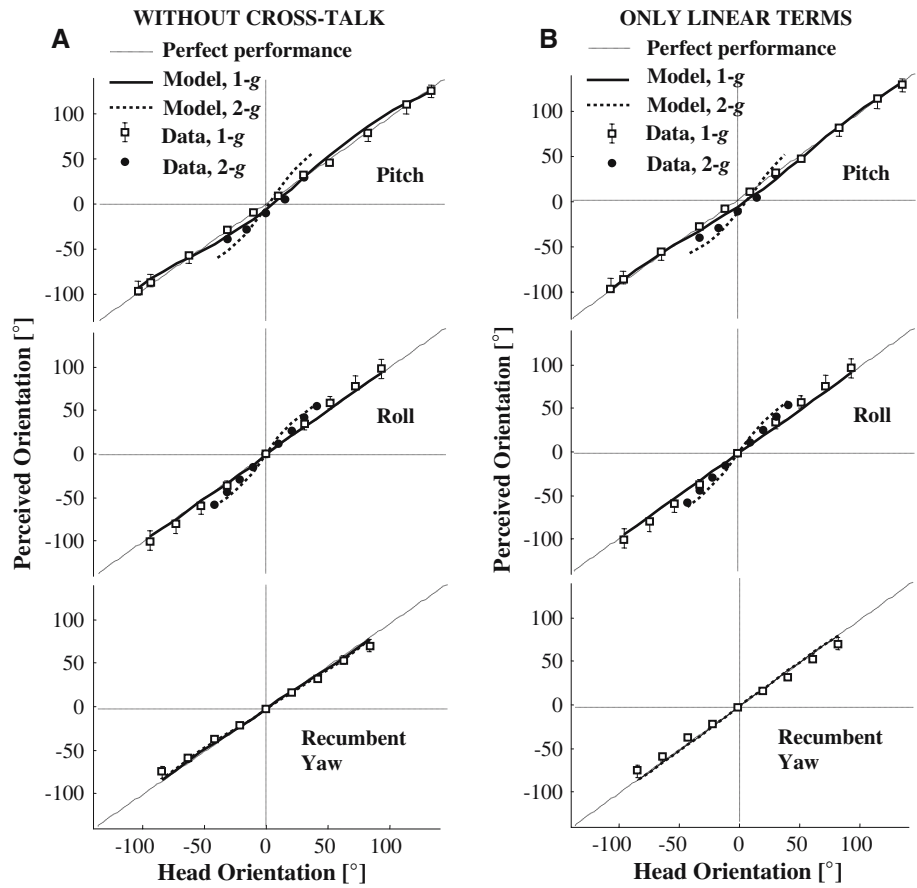

Fig. 9 Comparison of our static orientation model's predictions of performance of LD subjects with bilateral hypofunction. Data replotted from Graybiel and Clark (1965). The figure shows the compatibility of our model's postulations and Graybiel and Clark's findings

Fig. 10 Panel **a** shows how well our model fits experimental orientation data for the pitch, roll, and recumbent yaw axes when cross-talk coefficients are removed from the sensor model of Eq. 10 in the text. Panel **b** shows model performance when the non-linear components of the sensor model are omitted. The 2g data for roll and pitch performance are re-plotted from Correia et al. (1968) and Miller and Graybiel (1964)

WITHOUT CROSS-TALK

A
- Perfect performance
- **Model, 1-g**
- Model, 2-g
- Data, 1-g
- Data, 2-g

Pitch

Roll

Recumbent Yaw

ONLY LINEAR TERMS

B
- Perfect performance
- **Model, 1-g**
- Model, 2-g
- Data, 1-g
- Data, 2-g

Pitch

Roll

Recumbent Yaw

Perceived Orientation [°]

Head Orientation [°]

Scale factors for all three pairs of abscissa and ordinate axes could not possibly be predicted theoretically. We determined them numerically by identifying the coefficients of the matrices **A** and **B** and the exponent *n* of the mechanical model. Our non-linear system identification showed that making the **A** and **B** matrices symmetrical or asymmetrical (9 or 11 free parameters) led to the same fit because the off-diagonal (cross-talk) coefficients were always approximately equal. This suggests that the dimensionality of our model is 9 rather than 11. We also tried cases where the otolith model did not have the non-linear part or did not have cross-talk coefficients. The results of the respective fits are shown in Fig. 10a, b. The model still fits the data; the recumbent yaw estimate is still insensitive to the GIF magnitude; the pitch and roll errors for the 2 g conditions still have the proper magnitude; and, the position along the abscissa axis of the pitch error in 2g conditions is shown to be most affected by the cross-talk coefficients. Also, from comparing Figs. 5a, b, 10 we can conclude that the non-linear components of the input–output otolith model are responsible for the fine grained texture of the orientation errors, especially in 1g conditions. The off-diagonal terms of **A** and **B** (cross-talk coefficients) are responsible for the features of the pitch orientation errors.
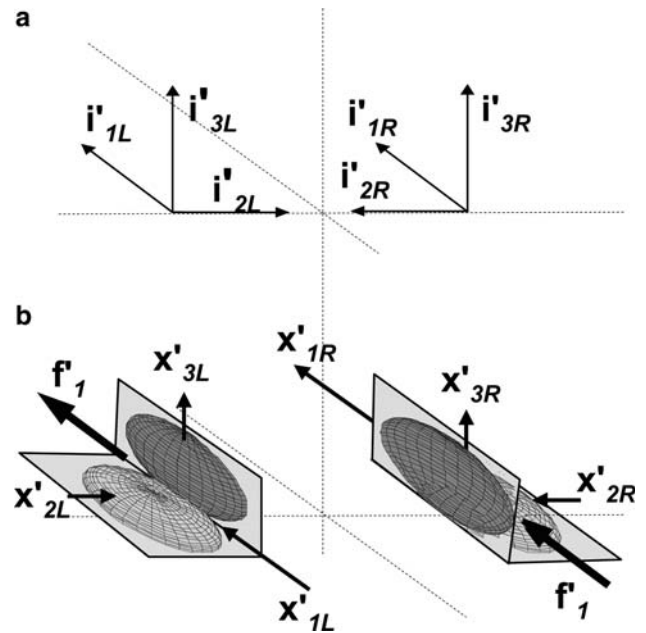
Fig. 11 a Reference frame and definition of variables for the right and left otolith organs and their respective arrangements; $\mathbf{f}' = (f'_1, f'_2, f'_3)$ represents the stimulus in otolith coordinates. The stimulus is the same on the left and right otoliths; however, the otoconial deflections are different for the left ($x'_{1L}, x'_{2L}, x'_{3L}$) and right ($x'_{1R}, x'_{2R}, x'_{3R}$) otoconia. **b** Schema of the cross-talks along the x'_2 and x'_3 axes produced by a stimulus (*thick arrow*) parallel to the $\mathbf{i}'_1$ axis. Forces along the other cardinal otolith axes would produce analogous cross-displacements in the respective orthogonal axes

Appendix

We model the otolith organs as if they were a single sensor located in the center of the head. The response of the combined sensor is the equal-weight sum or the difference of the signals coming from the right and left sides. The input to the sensor is the GIF ($\mathbf{f'}$) with its components expressed as f'_1, f'_2, and f'_3 in otolith coordinates. The natural orientation of $\mathbf{f'}$ is downward. The otolith organs individually are modeled as sets of three accelerometers capable of measuring the three components of the GIF (Fig. 11a). The response of the compound otolithic sensor $\tilde{\mathbf{x}}'$ is defined as $(\tilde{x}'_1, \tilde{x}'_2, \tilde{x}'_3)$, which is a function of $\mathbf{f'}$. The tilde symbol, $\sim$, indicates internal representations of the physical variables which are presented without the tilde.

Sensor errors affect perceived orientation. Possible error sources include, but are not limited to, crosstalk and non-linearity of the otolith response. Displacement of the otoconia can be proportional to the applied force in relation to a stiffness k value:

$$\tilde{x}' = \frac{f'}{k}$$

Linearity is rare in nature and generally does not extend over a broad range. Consequently, a more realistic way of addressing the mechanical characteristics of the otoliths is by introducing other terms in addition to the stiffness k:

$$\tilde{x}' = \frac{f'}{k} + \frac{(f')^n}{q}. \tag{11}$$

where $1/q$ is the coefficient of the nonlinear contribution ($n > 0$). Non-linearity contributes to orientation errors in the following manner. Two GIFs having the same direction but different magnitudes would, because of non-linearity, generate non-proportional sets of sensed/estimated variables $(\tilde{x}'_1, \tilde{x}'_2, \tilde{x}'_3)$ and therefore different perceived directions.

Cross-talk among sensor axes, e.g.,

$$\tilde{x}'_2 = \frac{f'_2}{k_{22}} + \frac{f'_3}{k_{23}}, \tag{12}$$

may produce sensor discharges in directions for which the GIF is not acting and consequently perception errors. An example of cross-talk is provided by Kondrachuk's (2001) finite element modeling of the deformation of the gel layer and the otolithic membrane of the utricle of the guinea pig in response to a static force stimulus. He demonstrated that the direction of displacement of a generic point of the utricle is not necessarily parallel to the direction of the applied force and that a force parallel to one axis can also elicit a displacement along the other two axes.

We treat the mechanical response of the otoliths within their own reference frame (Fig. 1a). To transform the stimulus force f from the head reference frame (Figs. 1a, 2, 3) to the otolith frame we multiply it by the following rotation matrix:

$$\mathbf{f'} \triangleq \mathbf{R}_y(-30)^\mathrm{T} \cdot \mathbf{f}; \ \mathbf{R}_y(-30)^\mathrm{T} = \begin{bmatrix} \cos 30° & 0 & \sin 30° \\ 0 & 1 & 0 \\ -\sin 30° & 0 & \cos 30° \end{bmatrix}. \tag{13}$$

Taking relationships 11, 12, and 13 into account for all three axes, we obtain the following comprehensive representation of the compound otolith sensor:

$$\tilde{x}'_1 = a_{11}f'_a + a_{12}f'_2 + a_{13}f'_3 + b_{11}(f'_1)^n + b_{12}(f'_2)^n + b_{13}(f'_3)^n$$
$$\tilde{x}'_2 = a_{21}f'_1 + a_{22}f'_2 + a_{23}f'_3 + b_{21}(f'_1)^n + b_{22}(f'_2)^n + b_{23}(f'_3)^n,$$
$$\tilde{x}'_3 = a_{31}f'_1 + a_{32}f'_2 + a_{33}f'_3 + b_{31}(f'_1)^n + b_{32}(f'_2)^n + b_{33}(f'_3)^n$$

which can be simplified as:

$$\tilde{\mathbf{x}}' = \mathbf{A}\mathbf{f'} + \mathbf{B}(\mathbf{f'})^n \tag{14}$$

The coefficients a_{ij} and b_{ij} are the "compliances"[6] of the i axis associated with the f'_i force.

The paired otolith organs are oriented opposite to each other along the inter-aural axis and in the same direction along the sagittal plane (cf. also Spoendlin 1965; Wilson and Melvill Jones 1979; see Fig. 11a). This layout is appropriate if the combined signal along the inter-aural axis ($\mathbf{i'}_2$) is the difference of the signals from the left and right otoliths (push–pull; cf. also Colenbrander 1964, Benson and Barnes 1970). Similarly, we can speculate that along the $\mathbf{i'}_1$ and $\mathbf{i'}_3$ axes the signals are the sums of signals of the two individual otoliths (pull–pull, cf. also Benson and Barnes 1970; Wilson and Melvill Jones 1979). Formally speaking, $\mathbf{x'} = (x'_{1L} + x'_{1R}, x'_{2L} - x'_{2R}, x'_{3L} + x'_{3R})$ represents the displacement of the combined otoconia. Hence, the inter-aural axis behaves symmetrically while the other two axes do not. In fact, along the inter-aural axis, at any given time, the stimulus on one utricle is just the opposite of that on the other (cf. Fig. 11a). Thus, whatever the response characteristics of a single utricle, the overall response of the pair, when combined, is symmetrical. Similar considerations apply to the saccule. Our experimental data for roll and recumbent yaw orientations also appear to be symmetrical, while the pitch data are not (Bortolami et al. 2006). This is consistent with the pull-pull signal configuration for the pitch axis, which is not necessarily bound to any symmetry.

Anatomical symmetries can help us identify potential patterns of cross-talk between mechanical axes. The sagittal plane is a plane of symmetry for the otolith organs. Figure 11b shows the pattern of dis-

---

[6]Compliances (reciprocals of stiffnesses) are properly defined as the coefficients of the matrix $\mathbf{A}$ when the model excludes the nonlinear part: $\tilde{\mathbf{x}}' = \mathbf{A}\mathbf{f'}$. In our analysis of compliance, the mechanical properties are expressed by the pair $\mathbf{A}$ and $\mathbf{B}$ together. We do not require non-negativity of the diagonals of $\mathbf{A}$, but rather the non-negativity of the total action of the diagonal terms of $\mathbf{A}$ and $\mathbf{B}$ together.

placements that would be produced by a force in the $\mathbf{i}'_1$ direction. The components along the stimulated axis yield the main response, which represents the diagonal terms of the matrices $\mathbf{A}$ and $\mathbf{B}$. The cross-talks, x'_{21} and x'_{31} relate to the coefficients (a_{21}, b_{21}) and (a_{31}, b_{31}) of the $\mathbf{A}$ and $\mathbf{B}$ matrices. The left and right contributions x'_{21L} and x'_{21R} are opposite to one another because of the symmetry of the two otoliths, but are equivalent in magnitude (at least in statistical terms, the otolith organs should have the same otoconial masses). Consequently, for the combined otoliths we obtain $x'_{21L} + x'_{21R} = x'_{21} \cong 0$. In turn, this implies $a_{21} = a_{21} = 0$ and $b_{21} = b_{21} = 0$. The same reasoning does not hold true for the x'_{31} component since x'_{31L} has the same sign as x'_{31R} which yields $a_{31} \neq 0$ and $b_{31} \neq 0$.

Figure 11a presents the pattern for the inter-aural axis. Along this axis the cross-talks are opposite in sign, which yields $a_{12} = b_{12} = a_{32} = b_{32} = 0$. Figure 11b shows the case for stimulation along the $\mathbf{i}'_3$ axis. Here, a_{23} and b_{23} will be equal to zero, while a_{13} and b_{13} will be different from zero. This analysis indicates that all off-diagonal coefficients of the matrices $\mathbf{A}$ and $\mathbf{B}$ besides the two pairs (a_{13}, b_{13}) and (a_{31}, b_{31}) must be statistically zero. Our formulation would therefore predict that during roll body reorientation there might also be a slight perception of pitch tilt (a_{13}, b_{13}). We have not yet experimentally looked for the presence of such effects but shall in the future. In conclusion, the structure of the model's matrices is as follows:

$$\mathbf{A} = \begin{bmatrix} a_{11} & 0 & a_{13} \\ 0 & a_{22} & 0 \\ a_{31} & 0 & a_{33} \end{bmatrix} \quad \mathbf{B} = \begin{bmatrix} b_{11} & 0 & b_{13} \\ 0 & b_{22} & 0 \\ b_{31} & 0 & b_{33} \end{bmatrix} \quad (15)$$

The values of the coefficients of $\mathbf{A}$ and $\mathbf{B}$ must be compatible with the fact that each axis cannot move opposite to the applied force. This can be formulated as follows (cf. also Fig. 6) and requires that the response should be monotonic within physiological ranges.

$$\sum_{j=1}^{3} a_{ij} f'_j + b_{ij} (f'_j)^n > 0; \quad i = 1 \dots 3$$

A least-squares algorithm (MATLAB™ 7.0: lsqnonlin) was used to determine the coefficients of $\mathbf{A}$ and $\mathbf{B}$ and the exponent n that best fit all of the experimental data for roll, pitch and recumbent yaw shown in Fig. 4. The model estimates the perceived vertical and not an Euler angle sequence of the head orientation. From the components of $\hat{\mathbf{g}}$, we derived roll, pitch and recumbent yaw projection angles. The derived angles $(\hat{\varphi}_R, \hat{\varphi}_P, \hat{\varphi}_Y)$ were compared against the experimental data to calculate the goodness of the prediction/fit. The least-squares algorithm then adjusted the matrices $\mathbf{A}$ and $\mathbf{B}$ and the exponent n until the fit did not improve with additional iterations.

We identified the coefficients of the model by both imposing (9 parameters) and not imposing (11 parame-ters) $a_{13} = a_{31}$ and $b_{13} = b_{31}$. Both led to comparable fits (Fig. 4). Further reduction of the number of parameters resulted in a worse fit as shown in Fig. 10. The identified characterization of the input–output model of the oto-lith (nine parameters) relative to the plots displayed in Figs. 5 and 6 is as follows:

$$\begin{Bmatrix} \tilde{x}'_1 \\ \tilde{x}'_2 \\ \tilde{x}'_3 \end{Bmatrix} = \begin{bmatrix} 1.7527 & 0 & -1.7268 \\ 0 & 2.5561 & 0 \\ -1.7268 & 0 & 1.7693 \end{bmatrix} \begin{Bmatrix} f'_1 \\ f'_2 \\ f'_3 \end{Bmatrix}$$
$$+ \begin{bmatrix} 0.6489 & 0 & 1.7450 \\ 0 & -0.5545 & 0 \\ 1.7450 & 0 & 0.5927 \end{bmatrix} \begin{Bmatrix} f'_1 \\ f'_2 \\ f'_3 \end{Bmatrix}^{1.5217}$$
(16)

The terms f'_i have dimensions of accelerations while the matrix coefficients, "compliances", have dimensions [s^2]. Finally, for clarity we report the flow chart of the actual implementation of the model.

$$\tilde{\mathbf{x}} = \mathbf{R}_y(30)^T \cdot \tilde{\mathbf{x}}'$$
$$\hat{\varphi}_{RP} = atan2\left(\left| \frac{f}{g} \right| \frac{\sqrt{\tilde{x}_1^2 + \tilde{x}_2^2}}{-\tilde{x}_3} \right)^7$$
$$\hat{\varphi}_Y = atan2\left(\frac{\tilde{x}_2}{\tilde{x}_1} \right)$$

These lead to the following estimates of the gravity vector with respect to the head:

$$\hat{g}_1 = \sin(\hat{\varphi}_{RP}) \cdot \cos(\hat{\varphi}_Y)$$
$$\hat{g}_2 = \sin(\hat{\varphi}_{RP}) \cdot \sin(\hat{\varphi}_Y)$$
$$\hat{g}_3 = -\cos(\hat{\varphi}_{RP})$$

This is the model output. However, to compare with the experimental data for the purpose of parameter identi-fication we used the following projection angles, which are not an Euler sequence.

$$\hat{\varphi}_R = atan2\left(\frac{-\hat{g}_2}{-\hat{g}_3} \right)$$
$$\hat{\varphi}_P = atan2\left(\frac{\hat{g}_1}{-\hat{g}_3} \right)$$
$$\hat{\varphi}_Y = atan2\left(\frac{\hat{g}_2}{-\hat{g}_1} \right)$$

The above representation is singular for $\hat{\mathbf{g}} \equiv (1, 0, 0)$, $\hat{\mathbf{g}} \equiv (0, 1, 0)$, and $\hat{\mathbf{g}} \equiv (0, 0, 1)$, for which the estimations of $\hat{\varphi}_R$, $\hat{\varphi}_P$, and $\hat{\varphi}_Y$ were extended for continuity.

---

[7] *Atan2* is the four-quadrant arctangent in MATLAB™ 7.0.

References

Angelaki DE, McHenry MQ, Dickman JD, Newlands SD, Hess BJM (1999) Computation of inertial motion: neural strategies to resolve ambiguous otolith information. J Neurosci 19:316–327

Bauermeister M, Werner H, Wapner S (1964) The effect of body tilt on tactual-kinesthetic perception of verticality. Am J Psychol 77:451–456

Benson AJ, Barnes GR (1970) Responses to rotating linear acceleration vectors considered in relation to a model of the otolith organs. In: The role of the vestibular organs in space exploration. NASA SP-314, pp 222–236

Bortolami SB, Pierobon A, DiZio P, Lackner JR (2006) Localization of the subjective vertical during roll, pitch and recumbent yaw body tilt. Exp Brain Res. DOI 10.1007/s00221-006-0385-y (current issue)

Bos J, Bles W (2002) Theoretical considerations on canal-otolith interaction and an observer model. Biol Cybern 86:191–207

Brown JL (1961) Orientation to the vertical during water immersion. Aerosp Med 32:209–217

Bryan AS, Ventura J, Bortolami SB, DiZio P, Lackner JR (2004) Localization of subjective vertical and head midline during recumbent yaw tilt in altered gravitoinertial force environments. Soc Neurosci Abst 868.1

Clark B, Graybiel A (1966) Factors contributing to the delay in the perception of the oculogravic illusion. Am J Psychol 79:377–388

Clark B, Graybiel A (1968) Influence of contact cues on the perception of the oculogravic illusion. Acta Otolaryngol 65:373–380

Colenbrander A (1964) Eye and otoliths. Aeromed Acta 9:45–91

Correia MJ, Hixson WC, Niven JI (1968) On predictive equations for subjective judgments of vertical and horizon in a force field. Acta Otolaryngol Suppl 230:1–20

Fernandez C, Goldberg JM, Abend WK (1972) Response to static tilts of peripheral neurons innervating otolith organs of the squirrel monkey. J Neurobiol 35:978–997

Glassauer S, Merfeld DM (1997) Modeling three dimensional vestibular responses during complex motion stimulation. In: Ketter M, Haslwanter T, Minslisch H, Tweed D (eds) Three dimensional kinematics of eye, head, and limb movements in health and disease. Harwood, Amsterdam, pp 387–398

Grant W, Best W (1987) Otolith-organ mechanics: lumped parameter model and dynamic response. Aviat Space Environ Med 58:970–976

Grant JW, Huang CC, Cotton JR (1994) Theoretical mechanical frequency response of the otolith organs. J Vestib Res 4:137–151

Graybiel A, Clark B (1965) Validity of the oculogravic illusion as a specific indicator of otolith function. Aerosp Med 36:1173–1180

Graybiel A, Patterson JL (1955) Thresholds of stimulation of the otolith organs as indicated by the oculogravic illusion. J Appl Physiol 7:666–670

Graybiel A, Miller EF, Newsom BD, Kennedy RS (1968) The effect of water immersion on perception of the oculogravic illusion in normal and labyrinthine-defective subjects. Acta Otolaryngol 65:599–610

Haslwanter T, Jaeger R, Mayr S, Fetter M (2000) Three-dimensional eye-movement responses to off-vertical axis rotations in humans. Exp Brain Res 134:96–106

Howard IP, Templeton WB (1966) Human spatial orientation. Wiley, London

Jarchow T, Mast FW (1999) The effect of water immersion on postural and visual orientation. Aviat Space Environ Med 70:879–886

Kalman RE (1960) A new approach to linear filtering and prediction problems. J Basis Eng 82:35–45

Kaptein RG, Van Gisbergen JA (2004) Interpretation of a discontinuity in the sense of verticality at large body tilt. J Neurophysiol 91:2205–2214

Kondrachuk AV (2001) Finite element modeling of the 3D otolith structure. J Vestib Res 11:13–32

Lackner JR (1992) Spatial orientation in weightless environments. Perception 656:329–399

Lackner JR, Graybiel A (1978a) Postural illusions experienced during z-axis recumbent rotation and their dependence upon somatosensory stimulation of the body surface. Aviat Space Environ Med 49:484–488

Lackner JR, Graybiel A (1978b) Some influences of touch and pressure cues on human spatial orientation. Aviat Space Environ Med 49:798–804

Lackner JR, Graybiel A (1979) Parabolic flight loss of sense of orientation. Science 206:1105–1108

Magnus R (1924) Körperstellung. Springer, Berlin Heidelberg New York

Maxwell SS (1923) Labyrinth and equlibrium. Saunders, Philadelphia

Mayne R (1950) The dynamic characteristics of the semicircular canals. J Comp Physiol 43:309–319

Mayne R (1974) Vestibular system part 2: psychophysics, applied aspects and general interpretations. In: Kornhuber HH (eds) Handbook of sensory physiology. Springer, Berlin Heidelberg New York, pp 494–580

Meiry JL (1966) The vestibular system and human dynamic space orientation. NASA

Meiry JL, Young LR (1967) Biophysical evaluation of the human vestibular system. In: Third Semi-Annual Status Report on NASA 1-14, Grant 22-009-156

Merfeld DM (1995) Modeling the vestibulo-ocular reflex of the squirrel monkey during eccentric rotation and roll tilt. Exp Brain Res 106:123–134

Merfeld DM, Zupan LH (2002) Neural processing of gravitoinertial cues in humans. III. Modeling tilt and translation responses. J Neurophysiol 87:819–833

Merfeld DM, Zupan LH, Peterka RJ (1999) Humans use internal models to estimate gravity and linear acceleration. Nature 398:615–618

Merfeld DM, Zupan LH, Gifford CA (2001) Neural processing of gravito-inertial cues in humans. II. Influence of the semicircular canals during eccentric rotation. J Neurophysiol 85:1648–1660

Miller EF, Graybiel A (1964) Magnitude of gravitoinertial force, an independent variable in egocentric visual localization of the horizontal. U.S. Naval School of Aviation Medicine, Pensacola, FL, Report No. 98, 31 July 1964

Miller EF, Fregly A, Graybiel A (1968) Visual horizontal perception in relation to otolith-function. Am J Psychol LXXXI:488–496

Mittelstaedt H, Fricke E (1988) The relative effect of saccular and somatosensory information on spatial perception and control. Adv Otorhinolaryngol 42:24–30

Mittlestaedt H (1983) A new solution to the problem of the subjective vertical. Naturwissenschaften 70:272–281

Murray RM, Zexiang L, Sastry SS (1994) A mathematical introduction to robotic manipulation. CRC Press, Boca Raton

Oman CM (1982) A heuristic mathematical model for the dynamics of sensory conflict and motion sickness. Acta Otolaryngol Suppl 392:1–44

Ormsby CC (1974) Model of human dynamic orientation. PhD Dissertation. M.I.T. 1-1-1974

Ormsby CC, Young LR (1976) Perception of static orientation in a constant gravitoinertial environment. Aviat Space Environ Med 47:159–164

Ormsby CC, Young LR (1977) Integration of semicircular canal and otolith information for multisensory orientation stimuli. Math Biosci 34:1–21

Savage PG (2000) Strapdown analytics. Strapdown Associates, Inc. Maple Plain

Schöne H (1964) On the role of gravity in human spatial orientation. Aerosp Med 35:764–772

Spoendlin HH (1965) Ultrastructural studies of the labyrinth in squirrel monkeys. NASA SP-77, Pensacola, pp 7–22

Van Beuzekom AD, Van Gisbergen JA (2000) Properties of the internal representation of gravity inferred from spatial-direction and body-tilt estimates. J Neurophysiol 84:11–27

Will CM (1981) Experimental test of Einstein equivalence principle. Theory and experimentation in gravitational theory. Cambridge University Press, Cambridge, p 27

Wilson VJ, Melvill Jones (1979) Mammalian vestibular physiology. Plenum, New York

Young LR, Meiry JL, Yao T Li (1966) Control engineering approaches to human dynamic space orientation. In: Role of vestibular organs in space exploration, NASA SP-115 U.S. Govt. printing office, Washington DC, pp 217–227

Zupan LH, Merfeld DM, Darlot C (2002) Using sensory weighting to model the influence of canal, otolith and visual cues on spatial orientation and eye movements. Biol Cybern 86:209–230